

Measurements of the Trilinear Gauge Boson Couplings from Diboson Production at DØ

J. Sekaric for the DØ Collaboration
 Department of Physics, Florida State University, Tallahassee, FL 32306-4350, USA

The most recent measurements of the trilinear gauge boson couplings from the diboson production at the DØ experiment has been presented. The analyzed final states are $Z\gamma \rightarrow \nu\nu\gamma$, $WW \rightarrow \nu l'\nu$, and $WW + WZ \rightarrow \nu jj$. We also present results obtained combining all final states involving the W boson. These results represent the most stringent limits set to date at the hadron collider.

1. Introduction

The simultaneous production of two vector bosons is a process of interest in many physics analysis at the Tevatron. Study of their production and interactions provide a test of the Electroweak Sector of the Standard Model (SM) either measuring their production cross sections or trilinear gauge boson couplings (TGCs) [1]. Any deviation from predicted SM values is an indication for New Physics (NP) beyond the SM and could give us some clues about the Electroweak Symmetry Breaking mechanism (EWSB).

2. Phenomenology

The TGCs contribute to diboson production via s -channel diagram. Thus, production of WW contains two trilinear γWW and ZWW gauge boson vertices while the WZ production contains the ZWW vertex only. The Effective Lagrangian which describes γ/ZWW vertices contains 14 charged coupling parameters [2]. They are grouped according to the symmetry properties into C (charge conjugation) and P (parity) conserving (g_1^V , κ_V , and λ_V), C and P violating but CP conserving (g_5^V), and CP violating (g_4^V , $\tilde{\kappa}_V$, and $\tilde{\lambda}_V$), where $V = Z, \gamma$. In the SM all couplings vanish ($g_5^V = g_4^V = \tilde{\kappa}_V = \tilde{\lambda}_V = \lambda_V = 0$) except $g_1^V = \kappa_V = 1$. The value of g_1^γ is fixed by electromagnetic gauge invariance ($g_1^\gamma = 1$) while the value of g_1^Z may differ from its SM value. Considering the C and P conserving couplings only, five couplings remain, and their deviations from the SM values are denoted as the anomalous TGCs $\Delta g_1^Z = (g_1^Z - 1)$, $\Delta\kappa_\gamma = (\kappa_\gamma - 1)$, $\Delta\kappa_Z = (\kappa_Z - 1)$, λ_γ and λ_Z . Charged TGCs g_1^Z , κ_γ and λ_γ relate to the W boson magnetic dipole moment μ_W and electromagnetic quadrupole moment q_W as:

$$\begin{aligned} \mu_W &= \frac{e}{2M_W}(g_1^\gamma + \kappa_\gamma + \lambda_\gamma), \\ q_W &= -\frac{e}{M_W^2}(\kappa_\gamma - \lambda_\gamma). \end{aligned} \quad (1)$$

In the $Z\gamma$ production, the $ZZ\gamma$ and $\gamma\gamma Z$ vertices contribute at the one-loop level or in the presence of NP but not at the tree-level. The Effective Lagrangian

contains 4 neutral coupling parameters h_i^V [3], where $V = Z, \gamma$ and $i = 1 - 4$. The h_1^V and h_2^V violate CP symmetry while h_3^V and h_4^V conserve CP symmetry and all four couplings are equal to zero in the SM. The couplings h_i^Z also relate to the magnetic and electric dipole and quadrupole moments of the Z boson [3], but they were not experimentally studied at the DØ experiment yet.

If anomalous TGCs are introduced in Effective Lagrangian, an unphysical increase in diboson production cross sections will result as the center-of-mass energy, $\sqrt{\hat{s}}$ approaches NP scale, Λ_{NP} . Such divergences would violate unitarity, but can be controlled by introducing a form factor $\Delta a(\hat{s}) = \Delta a_0 / (1 + \hat{s}/\Lambda_{NP}^2)^n$ for which the anomalous coupling vanishes as $\hat{s} \rightarrow \infty$. The coupling a_0 is a low-energy approximation of the coupling $a(\hat{s})$, $n = 2$ for γWW and ZWW couplings, $n = 3$ for h_1^V and h_3^V , $n = 4$ for h_2^V and h_4^V .

2.1. $Z\gamma \rightarrow \nu\nu\gamma$ Production

The $Z\gamma \rightarrow \nu\nu\gamma$ events are reconstructed from 3.6 fb⁻¹ of DØ data. Candidate events are required to have one isolated photon within pseudorapidity $|\eta_{det}| < 1.1$ [4], transverse energy $E_T > 90$ GeV and missing transverse energy $\cancel{E}_T > 70$ GeV. The pointing algorithm [5] which provides the matching of the electromagnetic shower to the primary vertex is used in order to reduce the contribution from bremsstrahlung photons. After all selection criteria were applied 51 $\nu\nu\gamma$ candidate events are observed. The predicted numbers of signal and background events are 33.7 ± 3.4 and 17.3 ± 2.4 , respectively. The dominant background events are $W \rightarrow e\nu$ in which the electron is misidentified as a photon and it contributes with 9.7 ± 0.6 events. The measured cross section is $\sigma_{ZZ} \times BR(Z \rightarrow \nu\nu) = 32 \pm 9$ (stat + syst) ± 2 (lumi) fb [6] which is in agreement with the next-to-leading (NLO) cross section of (39 ± 4) fb [7]. The observed signal significance is 5.1 standard deviations (s.d.). For the TGC studies, the photon E_T spectrum shown in Figure 1 is used to set the limits on $ZZ\gamma$ and $Z\gamma\gamma$ couplings. The Monte Carlo (MC) signal samples were generated with the leading-order (LO) $Z\gamma$

generator [8], corrected for the NLO effects with an E_T -dependent K factor [7] and passed through a parameterized simulation of the DØ detector. The signal templates with different anomalous TGC values are fitted to data in each bin of the photon E_T distribution, together with the SM background. The binned likelihood method [9] with the likelihood is used to extract the limits on TGCs from data.

The one-dimensional 95% C.L. limits for $h_{30,40}^{\gamma,Z}$ at $\Lambda_{NP} = 1.5$ TeV are $|h_{30}^{\gamma}| < 0.036$, $|h_{30}^Z| < 0.035$ and $|h_{40}^{\gamma,Z}| < 0.0019$ [6]. The combination with the previous 1 fb^{-1} data analysis in $ll\gamma$ final states [10] results in the most restrictive limits on these couplings at 95% C.L. of $|h_{30}^{\gamma,Z}| < 0.033$ and $|h_{40}^{\gamma,Z}| < 0.0017$. Three of them, h_{40}^{γ} , h_{40}^Z and h_{30}^Z , are world's best to date.

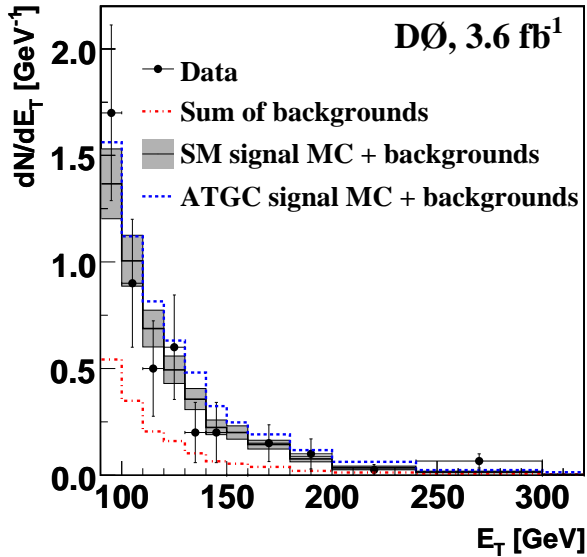


Figure 1: Photon E_T spectrum of $\nu\nu\gamma$ candidate events compared to the SM signal and background, and the expected distribution in the presence of anomalous TGCs. The systematic and statistical uncertainties on the SM MC events are included as shaded bands.

2.2. $WW \rightarrow l\nu l\nu$ Production

The most precise WW cross section measurement at the DØ experiment is performed analyzing the $l\nu l'\nu$ ($l, l' = e, \mu$) final states with 1.0 fb^{-1} of DØ data [11]. In each ll' final state ($ee, \mu\mu$ or $e\mu$) the two most energetic leptons are required to have $p_T > 25$ (15) GeV, to be of opposite charge and to be spatially separated from each other by $R > 0.8$ (ee) and $R > 0.5$ ($e\mu$). The $Z/\gamma^* \rightarrow ll$ background is effectively removed requiring $\cancel{E}_T > 45$ GeV (ee), 20 GeV ($e\mu$) or 35 GeV ($\mu\mu$), $\cancel{E}_T > 50$ GeV if $|M_Z - m_{ee}| < 6$ GeV (ee), $\Delta\phi_{\mu\mu} < 2.45$ and $\cancel{E}_T > 40$ GeV if $\Delta\phi_{e\mu} > 2.8$. Imposing the upper cut on the transverse momentum of the WW system, of 20 GeV (ee), 25 GeV ($e\mu$)

and 16 GeV ($\mu\mu$) minimizes the $t\bar{t}$ background. After all selection criteria were applied, all three combined channels yield 100 candidate events, 38.19 ± 4.01 predicted background events and 64.70 ± 1.12 predicted signal events. The cross section measurements in the individual channels are combined, yielding $\sigma_{WW} = 11.5 \pm 2.1$ ($stat+syst$) ± 0.7 ($lumi$) pb which is in agreement with the SM NLO prediction of 12.4 ± 0.8 pb [12]. The p_T distributions of the leading and trailing leptons (Figure 2) were used to set limits on anomalous

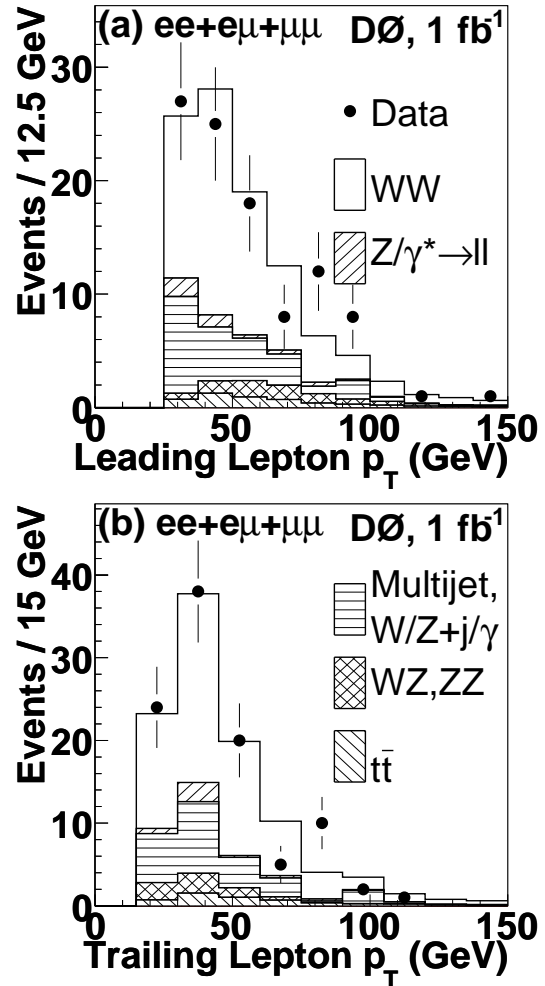


Figure 2: Distributions of the (a) leading and (b) trailing lepton p_T after final selection in $WW \rightarrow l\nu l'\nu$ analysis, combined for all channels ($ee + e\mu + \mu\mu$). Data are compared to estimated signal, and background sum.

TGCs, considering two different parameterizations between the couplings. Requiring $SU(2)_L \times U(1)_Y$ gauge symmetry [13] gives the following relationship between the TGC parameters: $\Delta\kappa_Z = \Delta g_1^Z - \Delta\kappa_\gamma \cdot \tan^2 \theta_W$ and $\lambda \equiv \lambda_Z = \lambda_\gamma$. Requiring equality between the $WW\gamma$ and WWZ vertices ($WW\gamma = WWZ$) [1] such that $\Delta\kappa \equiv \Delta\kappa_Z = \Delta\kappa_\gamma$ and $\lambda \equiv \lambda_Z = \lambda_\gamma$ and $g_1^Z = 1$ reduces the number of TGCs from three to two. We use the LO MC generator by Hagiwara, Woodside,

and Zeppenfeld (HWZ) [1, 2] to simulate the changes in WW production cross section and kinematics as TGCs are varied about their SM values. At each point in TGC space, generated events are passed through a parameterized simulation of the DØ detector. To increase the sensitivity to anomalous couplings, events are sorted by lepton p_T into a two-dimensional histogram. For each bin in lepton p_T space, the change in the number of WW events is parameterized by a quadratic function in $\Delta\kappa_\gamma$, λ_γ , Δg_1^Z space or in $\Delta\kappa$, λ space, depending on the TGC relation under study. In the first case, the third TGC parameter is fixed to its SM value. The likelihood values from MC to data fit are fitted with a 6th order polynomial and the limits are determined by integrating the likelihood curve and/or surface. The one-dimensional 95% C.L. limits for $\Lambda_{NP} = 2$ TeV are $-0.54 < \Delta\kappa_\gamma < 0.83$, $-0.14 < \lambda_\gamma = \lambda_Z < 0.18$ and $-0.14 < \Delta g_1^Z < 0.30$ under the $SU(2)_L \times U(1)_Y$ -conserving constraints, and $-0.12 < \Delta\kappa_\gamma = \Delta\kappa_Z < 0.35$ and $-0.14 < \lambda_\gamma = \lambda_Z < 0.18$ under the assumption that γWW and ZWW couplings are equal.

2.3. $WW + WZ \rightarrow l\nu jj$ Production

Using 1.1 fb^{-1} of DØ data the $l\nu jj$ ($l = e, \mu$) candidate events are selected requiring a single isolated lepton with $p_T > 20$ GeV and $|\eta| < 1.1$ (2.0) for electrons (muons), $\cancel{E}_T > 20$ GeV and at least two jets with $p_T > 20$ GeV [14]. The jet of highest p_T must have $p_T > 30$ GeV and the transverse mass of leptonically decaying W boson must be > 35 GeV to reduce the multijet background. Because of the small signal-to-background ratio (3%), an accurate modeling of the dominant W +jets background is essential and therefore, studied in great detail. After all selection criteria were applied, the signal and the backgrounds are further separated using a multivariate classifier, Random Forest (RF) [15] for purposes of the cross section measurement. The signal cross section is determined from a fit of signal and background RF templates to the data with respect to variations in the systematic uncertainties [16] and is measured to be $\sigma_{WW+WZ} = 20.2 \pm 2.5$ (stat) ± 3.6 (syst) ± 1.2 (lumi) pb which is consistent with the SM NLO prediction of $\sigma(WW + WZ) = 16.1 \pm 0.9$ pb [12]. The observed signal significance is 4.4 s.d.. The TGCs in $l\nu jj$ final states are measured from the dijet p_T distribution in the combined electron and muon channels shown in Figure 3. Data were compared to MC prediction with different anomalous TGC parameters. For this purpose we used the reweighting method to reweight the SM distribution to various anomalous TGC models [17] predicted by the HWZ generator using the weight R . This method is based on the fact that the differential cross section has a quadratic dependence on the anomalous couplings and can be

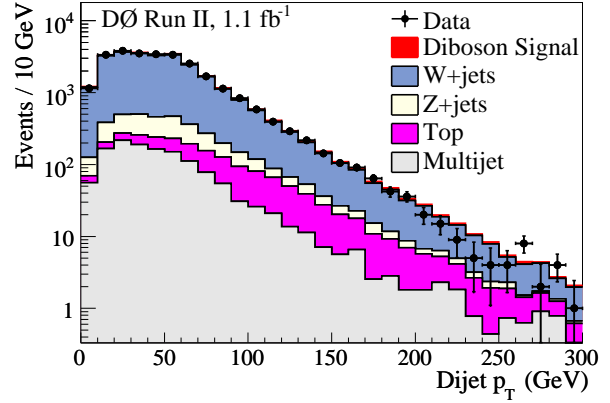


Figure 3: The dijet p_T distribution of combined (electron+muon) channels in the $WW + WZ \rightarrow l\nu jj$ analysis for data and SM predictions.

written as

$$\begin{aligned}
 d\sigma &= \text{const} \cdot |\mathcal{M}|^2 dX \\
 &= \text{const} \cdot |\mathcal{M}_{SM}^2| \frac{|\mathcal{M}|^2}{|\mathcal{M}_{SM}^2|} dX \\
 &= \text{const} \cdot |\mathcal{M}_{SM}^2| [1 + A(X)\Delta\kappa + B(X)\Delta\kappa^2 \\
 &\quad + C(X)\lambda + D(X)\lambda^2 + E(X)\Delta\kappa\lambda + \dots] dX \\
 &= d\sigma_{SM} \cdot R(X; \Delta\kappa, \lambda, \dots)
 \end{aligned} \tag{2}$$

where $d\sigma$ is the differential cross section that includes the contribution from the anomalous couplings, $d\sigma_{SM}$ is the SM differential cross section, $|\mathcal{M}|^2$ is the matrix element squared in the presence of anomalous couplings, $|\mathcal{M}_{SM}^2|$ is the matrix element squared in the SM, X is a kinematic distribution sensitive to the anomalous couplings and $A(X)$, $B(X)$, $C(X)$, $D(X)$, and $E(X)$ are reweighting coefficients dependent on X . In the $SU(2)_L \times U(1)_Y$ scenario R is parametrized with the three couplings Δg_1^Z , $\Delta\kappa_\gamma$, λ and nine reweighting coefficients, $A(X) - I(X)$ while in the $WW\gamma = WWZ$ scenario R is parametrized with the two couplings $\Delta\kappa$, λ and five reweighting coefficients, $A(X) - E(X)$. The kinematic variable X is chosen to be the p_T of the $q\bar{q}$ system, which is highly sensitive to anomalous TGCs. To get signal MC templates with different anomalous TGCs, each event in a reconstructed dijet p_T bin is weighted by the appropriate weight R and all the weights are summed in that bin. The observed limits are determined from a Poisson χ^2 fit of background and reweighted signal MC distributions for different anomalous couplings contributions to the observed data with respect to variations to the systematic uncertainties [16] using the dijet p_T distribution of candidate events. For the $SU(2)_L \times U(1)_Y$ scenario, the most probable coupling values as measured in data with associated uncertainties at 68% C.L. are $\kappa_\gamma = 1.07^{+0.26}_{-0.29}$, $\lambda = 0.00^{+0.06}_{-0.06}$, and $g_1^Z = 1.04^{+0.09}_{-0.09}$. For the $WW\gamma = WWZ$ scenario the most probable coupling values as measured in data with associated uncertainties at 68% C.L. are

$SU(2)_L \times U(1)_Y$ scenario	$\Delta\kappa_\gamma$	$\lambda = \lambda_\gamma = \lambda_Z$	Δg_1^Z
$WZ \rightarrow \ell\nu\ell\ell$ (1 fb ⁻¹)	-	$-0.17 < \lambda < 0.21$	$-0.14 < \Delta g_1^Z < 0.34$
$W\gamma \rightarrow \ell\nu\gamma$ (0.7 fb ⁻¹)	$-0.51 < \Delta\kappa_\gamma < 0.51$	$-0.12 < \lambda < 0.13$	
$WW \rightarrow \ell\nu\ell'\nu$ (1 fb ⁻¹)	$-0.54 < \Delta\kappa_\gamma < 0.83$	$-0.14 < \lambda < 0.18$	$-0.14 < \Delta g_1^Z < 0.30$
$WW + WZ \rightarrow \ell\nu jj$ (1.1 fb ⁻¹)	$-0.44 < \Delta\kappa_\gamma < 0.55$	$-0.10 < \lambda < 0.11$	$-0.12 < \Delta g_1^Z < 0.20$
$WW\gamma = WWZ$ scenario	$\Delta\kappa_\gamma$	$\lambda = \lambda_\gamma = \lambda_Z$	Δg_1^Z
$WZ \rightarrow \ell\nu\ell\ell$ (1 fb ⁻¹)		$-0.17 < \lambda < 0.21$	
$W\gamma \rightarrow \ell\nu\gamma$ (0.7 fb ⁻¹)		$-0.12 < \lambda < 0.13$	
$WW \rightarrow \ell\nu\ell'\nu$ (1 fb ⁻¹)	$-0.12 < \Delta\kappa < 0.35$	$-0.14 < \lambda < 0.18$	
$WW + WZ \rightarrow \ell\nu jj$ (1.1 fb ⁻¹)	$-0.16 < \Delta\kappa < 0.23$	$-0.11 < \lambda < 0.11$	

Table I Comparison of 95% C.L. one-parameter TGC limits between the different channels studied at DØ with ≈ 1 fb⁻¹ of data: $WW \rightarrow \ell\nu\ell'\nu$, $W\gamma \rightarrow \ell\nu\gamma$, $WZ \rightarrow \ell\ell\nu$ and $WW + WZ \rightarrow \ell\nu jj$ ($l = e, \mu$) at $\Lambda_{NP} = 2$ TeV.

$\kappa = 1.04_{-0.11}^{+0.11}$ and $\lambda = 0.00_{-0.06}^{+0.06}$. The observed 95% C.L. limits estimated from the single parameter fit are $-0.44 < \Delta\kappa_\gamma < 0.55$, $-0.10 < \lambda < 0.11$, and $-0.12 < \Delta g_1^Z < 0.20$ for the $SU(2)_L \times U(1)_Y$ scenario or $-0.16 < \Delta\kappa < 0.23$ and $-0.11 < \lambda < 0.11$ for the $WW\gamma = WWZ$ scenario. Table I shows the comparison of the 95% C.L. limits on charged anomalous couplings set from data in different DØ diboson analyses.

This analysis yields the most stringent limits on $\gamma WW/ZWW$ anomalous couplings from the Tevatron to date, complementing similar measurements performed in fully leptonic decay modes from $W\gamma$, WW , and WZ production.

3. Combined Study of TGCs

Finally, we combined four different diboson analyses, $WW \rightarrow \ell\nu\ell'\nu$, $WZ \rightarrow \nu lll$ [18], $W\gamma \rightarrow \ell\nu\gamma$ [19] and $WW + WZ \rightarrow \ell\nu jj$, to set the limits on charged couplings using 0.7-1 fb⁻¹ of DØ data. The kinematic distributions sensitive to anomalous TGCs are the photon E_T spectrum in $W\gamma$ analysis and the Z boson p_T spectrum in WZ analysis, shown in Figure 4. The lepton p_T distributions and dijet p_T distribution are used as an input from $WW \rightarrow \ell\nu\ell'\nu$ and $WW + WZ \rightarrow \ell\nu jj$ analyses, respectively. Two different relations between anomalous TGCs, $SU(2)_L \times U(1)_Y$ and $WW\gamma = WWZ$, has been considered for $\Lambda_{NP} = 2$ TeV.

Combined 95% C.L. limits in both scenarios represent an improvement of about a factor of 3 relative to the previous DØ [20] and CDF [21] results and they are shown in Table II. These are the tightest limits to date on $\Delta\kappa_\gamma$, λ_γ and Δg_1^Z couplings at the hadron collider. The 68% C.L. limits are presented in Table II

as well. With only 1 fb⁻¹ of data the sensitivity obtained at the 68% C.L. is comparable to that of an individual LEP2 experiment.

We also measure the W boson magnetic dipole and electric quadrupole moments respecting $SU(2)_L \otimes U(1)_Y$ symmetry with $g_1^Z = 1$. Their measured values and the one-dimensional 68% C.L. intervals are $\mu_W = 2.02_{-0.09}^{+0.08}$ ($e/2M_W$) and $q_W = -1.00 \pm 0.09$ (e/M_W^2), respectively. This is the most stringent published result of μ_W and q_W moments [22].

Limits for $SU(2)_L \otimes U(1)_Y$ scenario			
Parameter	Minimum	68% C.L.	95% C.L.
$\Delta\kappa_\gamma$	0.07	[-0.13, 0.23]	[-0.29, 0.38]
Δg_1^Z	0.05	[-0.01, 0.11]	[-0.07, 0.16]
λ	0.00	[-0.04, 0.05]	[-0.08, 0.08]
Limits for $WW\gamma = WWZ$ scenario			
Parameter	Minimum	68% C.L.	95% C.L.
$\Delta\kappa$	0.03	[-0.04, 0.11]	[-0.11, 0.18]
λ	0.00	[-0.05, 0.05]	[-0.08, 0.08]

Table II The most probable TGC values and one-dimensional 68% and 95% C.L. intervals on anomalous values of γWW and ZWW TGCs from the combined fit of $\ell\nu\gamma$, $\ell\nu\ell'\nu$, νlll and $\ell\nu jj$ final states.

4. Conclusions

The most recent measurements of the TGCs at the DØ experiment has been presented. No deviation from the SM prediction has been observed. The DØ experiment sets the world's tightest limits on neutral couplings $h_{30}^{Z,\gamma}$ and h_{40}^γ in $Z\gamma \rightarrow \nu\nu\gamma$ analysis. The limits set on Δg_1^Z , $\Delta\kappa_\gamma$ and λ_γ in the $\ell\nu jj$ final states are the stringent limits at the hadron collider

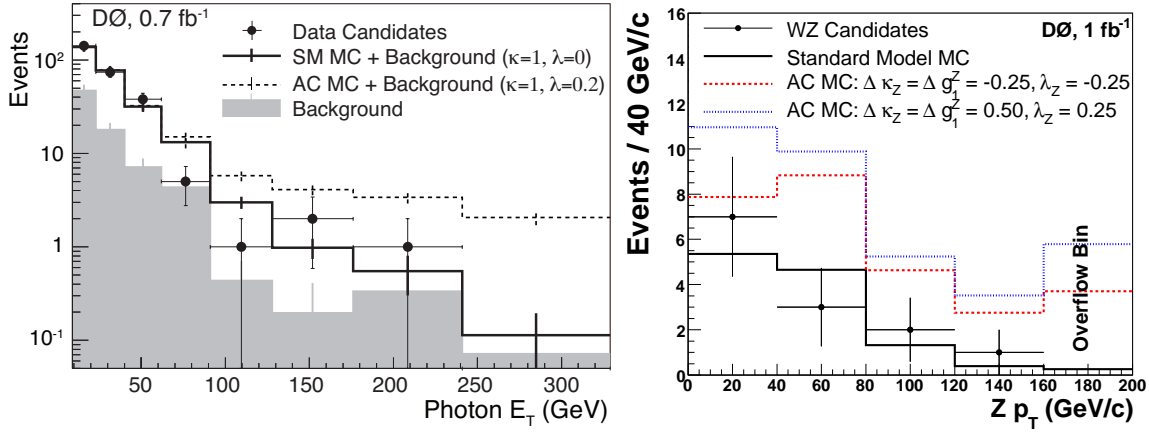


Figure 4: Left: The photon E_T spectra for the SM (solid line), an anomalous TGC point (dashed line), combined electron and muon channel data candidates (black points), and the background estimate (shaded histogram) from the $W\gamma$ analysis. Right: The reconstructed Z boson p_T of the WZ candidate events. The solid histogram is the expected sum of signal and background in the SM and the black dots represent the data. The dotted and double dotted histograms are the expected sums of signal and background for two different cases of anomalous TGCs.

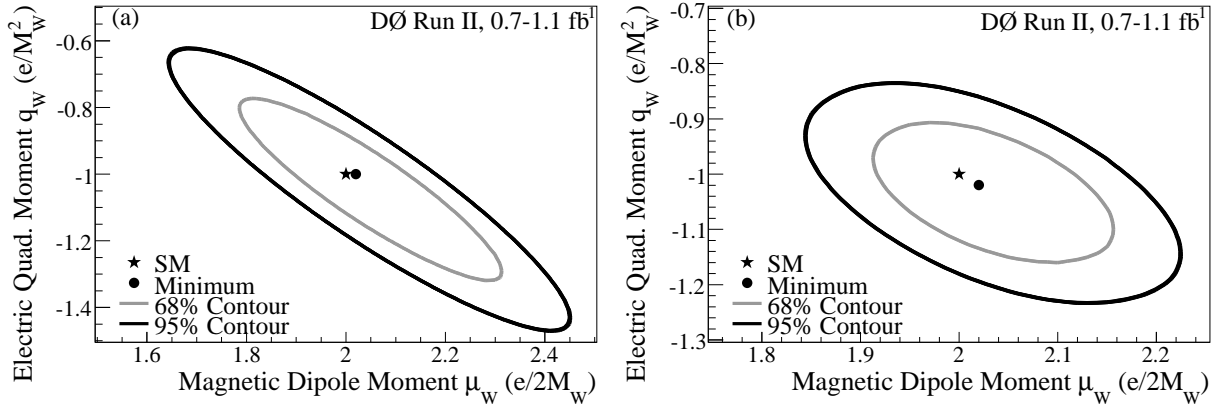


Figure 5: Two-dimensional 68% and 95% C.L. limits for the W boson electric quadrupole moment vs. the magnetic dipole moment (a) when respecting $SU(2)_L \times U(1)_Y$ symmetry and (b) when respecting $WW\gamma = WWZ$ constraints. In both cases we assume $\Lambda_{NP} = 2$ TeV.

obtained from only one final state. The combination of $\nu\nu\gamma$, $\nu\nu'\nu$, νlll and νljj final states, results in the tightest limits on charged TGCs at the hadron collider to date, significantly approaching to individual LEP2 sensitivities. We also present the world's best results on the W boson magnetic dipole and electromagnetic quadrupole moments.

Acknowledgments

We thank the staffs at Fermilab and collaborating institutions, and acknowledge support from the DOE and NSF (USA); CEA and CNRS/IN2P3 (France); FASI, Rosatom and RFBR (Russia); CNPq, FAPERJ, FAPESP and FUNDUNESP (Brazil); DAE and DST (India); Colciencias (Colombia); CONACyT (Mexico); KRF and KOSEF (Korea); CONICET and UBA-

CyT (Argentina); FOM (The Netherlands); STFC and the Royal Society (United Kingdom); MSMT and GACR (Czech Republic); CRC Program, CFI, NSERC and WestGrid Project (Canada); BMBF and DFG (Germany); SFI (Ireland); The Swedish Research Council (Sweden); and CAS and CNSF (China).

References

- [1] K. Hagiwara, J. Woodside, and D. Zeppenfeld, *Phys. Rev. D* **41**, 2113 (1990).
- [2] K. Hagiwara *et al.*, *Nucl. Phys. B* **282**, 253 (1987).
- [3] J. Ellison and J. Wudka, *Annu. Rev. Nucl. Part. Sci.* **48**, 33 (1998).

- [4] DØ uses a cylindrical coordinate system with the z axis running along the beam axis. Angles θ and ϕ are the polar and azimuthal angles, respectively. Pseudorapidity is defined as $\eta = -\ln[\tan(\theta/2)]$ in which θ is measured with respect to the primary vertex. In the massless limit, η is equivalent to the rapidity $y = (1/2)\ln[(E + p_z)/(E - p_z)]$. η_{det} is the pseudorapidity measured with respect to the center of the detector.
- [5] S. Kesisoglou, FERMILAB-THESES-2004, UMI-31-74625 (2004).
- [6] DØ Collaboration: V. M. Abazov *et al.*, *Phys. Rev. Lett.* **102**, 201802 (2009).
- [7] U. Baur, T. Han and J. Ohnemus, *Phys. Rev. D* **57**, 2823 (1998).
- [8] U. Baur and E. L. Berger, *Phys. Rev. D* **47**, 4889 (1993).
- [9] The DØ Collaboration: S. Abachi *et al.*, *Phys. Rev. D* **56**, 6742 (1997). See Appendix B.
- [10] The DØ Collaboration: V. M. Abazov *et al.*, *Phys. Lett. B* **653**, 378 (2007).
- [11] DØ Collaboration: V. M. Abazov *et al.*, FERMILAB-PUB-09-094-E, accepted by *Phys. Rev. Lett.* (2009).
- [12] J. M. Campbell and R. K. Ellis, *Phys. Rev. D* **60**, 113006 (1999). Cross sections were calculated with the same parameter values given in the paper, except with $\sqrt{s} = 1.96$ TeV.
- [13] A. De Rujula, M. B. Gavela, P. Hernandez and E. Masso, *Nucl. Phys. B* **384**, 3 (1992); M. Bilenky, J. L. Kneur, F. M. Renard and D. Schildknecht, *Nucl. Phys. B* **409**, 22 (1993).
- [14] DØ Collaboration: V. M. Abazov *et al.*, *Phys. Rev. Lett.* **102**, 161801 (2009).
- [15] L. Breiman, *Machine Learning* **45**, 5 (2001); I. Narsky, arXiv:physics/0507143 [physics.data-an] (2005).
- [16] W. Fisher, FERMILAB-TM-2386-E (2006).
- [17] DØ Collaboration: V. M. Abazov *et al.*, *Phys. Rev. D* **80**, 053012 (2009).
- [18] DØ Collaboration, V. M. Abazov *et al.*, *Phys. Rev. D* **76**, 111104(R) (2007).
- [19] DØ Collaboration, V. M. Abazov *et al.*, *Phys. Rev. Lett.* **100**, 241805 (2008).
- [20] DØ Collaboration: B. Abbott *et al.*, *Phys. Rev. D* **60**, 072002 (1999).
- [21] CDF Collaboration: T. Aaltonen *et al.*, *Phys. Rev. D* **76**, 111103(R) (2007).
- [22] DØ Collaboration: B. Abazov *et al.*, FERMILAB-PUB-09-380-E, submitted to *Phys. Lett. B* (2009).